Solar Induced Bending Vibrations of a Flexible Member

JOHN D. GRAHAM*
Star Aerospace Products Ltd., Malton, Ontario, Canada

The stability of in-plane bending oscillations of long flexible members (STEMs) when subjected to solar heating is examined. The model accounts for the interdependence between the time varying STEM thermal curvature (caused by its changing temperature distribution) and the STEM bending motion. The linearized response of the STEM is determined in the Laplace transformed time domain and the ensuing stability criterion is found to be dependent upon, along with other parameters, the sun orientation, the material surface absorptivity and the extent of damping in the STEM, the latter being due mainly to the friction in the overlapped or interlocked part of the STEM element. In the case where the STEM is oriented towards the sun the motion is shown to be stable. The use of the best available values of absorptivity and damping shows stability to be marginal for silver-plated STEM in the case where the STEM is oriented away from the sun. More accurate test information on the mechanism and magnitude of damping is required to accurately determine stability or otherwise in the latter case.

Nomenclature

A = see Eq. (13) and Fig. 3
a_{nm}, b_{nm} = see Eqs. (32), (35)
C_n = see Eq. (34)
C = specific heat of STEM material
EI = bending stiffness of STEM section
e_c = coefficient of thermal expansion
$f_n(\tau)$ = time varying part of u
$f_n(s)$ = Laplace transform of $f_n(\tau)$
H = time independent part of temperature differential
H_o = approximate average temperature
h = see Eq. (5)
J = time varying part of temperature differential
$\bar{J}$ = Laplace transform of J
k = conductivity
K_t = thermal curvature
K_1 = time independent part of thermal curvature
K_2 = time varying part of thermal curvature
K_o = see Eq. (17)
l = length
M_D = damping moment
M_x = bending moment at section x
m_D = damping moment per unit length
r = radius
R = radius of curvature
S = solar radiation constant
T = temperature
T_1 = temperature differential
t = STEM material thickness
$u(x,\tau)$ = see Eq. (24)
$u(\phi)$ = see Eq. (1)
V = static thermal deflection; see (20)
w = total deflection
W = time varying part of deflection
x = undeflected STEM axis
$X_n(y)$ = characteristic function; see (29)
y = $l - x$
α = solar absorptivity
β = slope in static thermally deflected shape
δ_s = element of stem length
ϵ = emissivity
ζ = damping constant
η = damping parameter, see (18)
η_1 = damping parameter, see (37)
Θ = see Eq. (11)
θ = slope change due to bending oscillation
θ_0 = amplitude of θ
λ = angle between sun vector and STEM normal; see Fig. 1
λ_0 = angle between sun vector and STEM normal when not deflected
μ = mass per unit length
ρ = STEM material density
σ = Stefan-Boltzmann constant
τ = time
Φ = angle of curvature
ϕ = angular coordinate around STEM
ω = frequency
ω_n = resonant frequency of nth bending mode
ξ = $k/c\rho r^2$
ψ = $S\alpha/c\rho t$

Subscripts and superscripts

m,n = mode number; see Eq. (32)
$'$ = differentiation with respect to y
$\cdot$ = differentiation with respect to τ

Received April 3, 1969; revision received December 15, 1969. Part of the support for this work was provided by DIR Grant 5540/33 from the Defence Research Board of Canada.

* Head, Systems Analysis; also Research Associate, Institute of Aerospace Studies, University of Toronto, Toronto, Ontario, Canada. Member AIAA.

Introduction

A NUMBER of references[1-4] have discussed thermal flutter problems associated with satellites having long flexible members or STEMs[6] which change their sun orientation slowly. The physical basis for such an instability has been explained to a large extent by Donohue and Frisch[1] and at least two simulation studies have been carried out[5,7] to predict motions where characteristics agree with observed motions.

The motion has been attributed to the very low torsional stiffness of conventional STEMs and Donohue[1] has shown that such STEMs, when exposed to the sun, will oscillate in a mode combining twisting and bending in a plane perpendicular to the sun direction. Unpublished work by the present author[8] has also shown that the uncoupled linearized twist response of such STEMs exhibits instabilities.

This problem has led to much work by STEM manufacturers aimed at developing STEMs with a high torsional stiffness, obtained by interlocking the overlapped edges. Such a section will have a torsional stiffness approaching that of a closed circular section.[9] The ratio of torsional stiffness for such a closed section is typically 1000 times that of an open section and so it would be expected that such sections would not be subject to the above thermal flutter problem.

However, Yu[10] has predicted that, even with a STEM of high torsional stiffness, in plane bending instabilities can

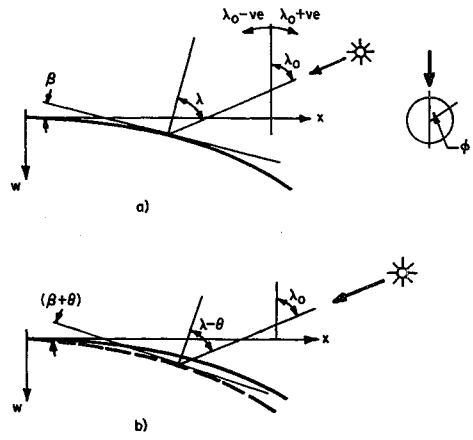

Fig. 1 STEM: a) in static thermally deflected position; and b) in oscillation about this position.

occur when the STEM is exposed to sunlight. Unfortunately, as is shown in this report, approximations made to boundary conditions have lead to errors in his stability criteria.

In this work an expression for the time varying temperature distribution throughout the STEM and the resulting thermal curvature as a function of STEM motion is developed. The time varying thermal curvature is then incorporated into the bending dynamics of the STEM and the stability of the resulting linearized motion is examined. It is found that an unstable motion is possible if the STEM points away from the sun, the stability being dependent upon sun orientation, material surface absorptivity, and the damping inherent in the STEM. The most important damping mechanism is that due to the friction between the overlapping parts of the STEM section. The use of the "best" available value of damping shows the stability to be marginal for silver plated STEM and predicts unstable conditions for all but short lengths of unplated STEM.

Stem Temperature Distribution

In Ref. 11 there is obtained the static temperature distribution in a long circular STEM subjected to solar radiation. Reference 12 finds the static temperature distribution in such a STEM with overlap. In the application with which this paper deals there is required the time varying part of the temperature distribution due to the STEM motion. This leads to the time varying thermal curvature which is the exciting mechanism for the oscillation being investigated. The assumptions made in the present heat-transfer analysis are as follows. 1) Thermal conduction along the length of the STEM is neglected. 2) The wall thickness of the STEM is so small that there is no temperature gradient across it. 3) Internal radiation between opposite walls of the STEM has a negligible effect in reducing temperature gradients compared with the effects of conduction around the STEM. 4) The STEM is considered as being a closed circular section so that conduction is uniform around it. The latter is not really the case with an interlocked STEM since the thermal conduction will be reduced at the interlock. However, the assumption leads to simplicity in analysis and, if a particular interlocked section is used in an application, the temperature distribution and the resulting thermal curvature will need to be modified accordingly.

Figures 1a and 1b show the situation considered where the cantilevered STEM is considered to be oscillating about its equilibrium position. The equilibrium position at distance x from the root is defined by the angle λ (which is a function of x) and the STEM is oscillating about this equilibrium position and instantaneously is defined by the angle $(\lambda - \theta)$. At an angle ϕ around the section at x the local normal to the surface makes an angle with the sun vector given by the inverse cosine of $[\cos\phi \cos(\lambda - \theta)]$ and the solar heat input at a small element at this point is reduced below its maximum by this factor for $\phi < \pi/2$. For $\phi > \pi/2$ the section is not exposed to the sun and there is no solar heat input. The instantaneous equation of heat transfer for an element $tr\delta\phi\delta x$ (see Fig. 2) for a time period $\delta\tau$ is

$$\begin{aligned}\text{Increase in Element} &= \text{Heat Radiated In} + \text{Heat Conducted In}\\ \text{Internal Energy} &- \text{Heat Radiated Out} - \text{Heat Conducted Out}\end{aligned}$$

$$c\rho\delta T r\delta\phi t\delta x = u(\phi)S\alpha r\delta\phi\delta x\delta\tau \cos\phi \cos(\lambda - \theta) - kt\delta x(\partial T/r\partial\phi)_{\phi}\delta\tau - \epsilon\sigma r\delta\phi\delta x\delta\tau T^4 + kt\delta x\delta\tau(\partial T/r\partial\phi)_{\phi+}$$

This can be simplified to the differential equation

$$\partial T/\partial\tau - \xi\delta^2 T/\partial\phi^2 + \epsilon\sigma T^4/c\rho t = \psi u(\phi) \cos\phi \cos(\lambda - \theta) \quad (1)$$

where $u(\phi) = 1$ in the top hemisphere (see Fig. 1) and $u(\phi) = 0$ in the bottom hemisphere. A similar equation can be written for $T(\pi - \phi)$ namely

$$\partial T(\pi - \phi)/\partial\tau - \xi\partial^2 T(\pi - \phi)/\partial\phi^2 + \epsilon\sigma T^4(\pi - \phi)/c\rho t = -\psi u(\pi - \phi) \cos\phi \cos(\lambda - \theta) \quad (2)$$

where $u(\pi - \phi) = 1$ in the bottom hemisphere and $u(\pi - \phi) = 0$ in the top hemisphere. By subtracting (2) from (1) the step functions are eliminated and there is obtained

$$\partial T_1/\partial\tau - \xi\partial^2 T_1/\partial\phi^2 + hT_1 = \psi \cos\phi \cos(\lambda - \theta) \quad (3)$$

where

$$T_1(\phi,\tau) = T(\phi,\tau) - T(\pi - \phi,\tau) \quad (4)$$

and

$$h = [T^2(\pi - \phi) + T^2(\phi)][T(\pi - \phi) + T(\phi)]\epsilon\sigma/c\rho t$$

Since for all practical cases the temperature differential across the STEM is much smaller than the absolute STEM temperature h can be approximated to a constant independent of ϕ and τ

$$h = 4\epsilon\sigma H_0^3/c\rho t \quad (5)$$

H^4 being the approximate average STEM temperature.

Recognizing that $T_1 = 0$ at $\phi = \pm\pi/2$ and that T_1 is symmetric about $\phi = 0$ then the form of (3) indicates that

$$T_1(\phi,\tau) = T_2(\tau) \cos\phi \quad (6)$$

From substituting (6) in (3)

$$nT_2/d\tau + (h + \xi)T_2 = \psi \cos(\lambda - \theta) \quad (7)$$

Equation (7) indicates that T_2 can be written in terms of a constant and time varying term, namely

$$T_2 = H + J(\tau) \quad (8)$$

where

$$H = \psi \cos\lambda/(h + \xi) \quad (9)$$

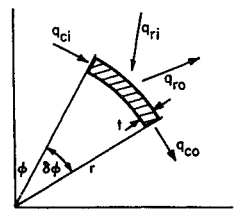

Fig. 2 Major heat transfer mechanisms operating in STEM.

and

$$dJ/d\tau + (h + \xi)J = \psi[\sin\lambda \sin\theta - \cos\lambda(1 - \cos\theta)] \quad (10)$$

For purposes of later use the Laplace transform is taken of Eq. (10) leading to

$$\bar{J}(s) = \psi\Theta(s)/(s + h + \xi) \quad (11)$$

$\Theta(s)$ being the transform of the bracketed term in Eq. (10)

Stem Thermal Curvature

From (6) and (7)

$$T_1(\tau,\phi) = \cos\phi[H + J(\tau)] \quad (12)$$

This temperature differential is related to the curvature at the section. Equation (12) shows that the temperature differential and hence the resulting thermal expansion is linearly proportional to the distance from the neutral axis. From Fig. 3, where A replaces $H + J(\tau)$

$$K_T = 1/R = \Phi/\delta s$$

and $\Phi = \delta_s e_c A/2r$. So

$$K_T(\tau) = e_c[H + J(\tau)]/2r \quad (13)$$

This comprises a steady thermal curvature K_1 and a time varying curvature K_2 corresponding, respectively, to the first and second terms of (13).

It is useful to determine this thermal curvature when a small sinusoidal oscillation of θ is occurring. In particular, assume the oscillation

$$\theta = \theta_0 \sin\omega\tau \quad (14)$$

Because θ is small Eqs. (10) and (11) show that

$$\Theta(S) = \theta(S) \sin\lambda \quad (15)$$

and on using this in Eq. (11) and transforming back to the time domain, the steady-state part of the solution is

$$K_T(\tau) = K_0 \cos\lambda + K_0 \sin\lambda[\theta - \dot{\theta}/(h + \xi)]/[1 + \{\omega/(h + \xi)\}^2] \quad (16)$$

where

$$K_0 = \psi e_c/2r(h + \xi) \quad (17)$$

The $\dot{\theta}$ term in Eq. (16) shows that the time varying part of the thermal curvature lags behind what it would be at a steady displacement θ and also that the magnitude of this part of the curvature is reduced by the factor $[1 + \{\omega/(h + \xi)\}^2]$. The former is important as it determines the stability of the motion and the latter determines the degree of stability (or instability). Both these points will be discussed later.

Discussion of Damping

Damping in STEMs, as in many other structures, is a complex phenomenon which is quite difficult to model accurately. Likins[15] has introduced it in an ad hoc manner into the time dependent vibration equation after separating the spatial dependence. Zener[16] has developed a theory for viscoelastic damping which, if applied to STEMs, does give small damping. The only published tests on damping of STEMs is that reported by Predmore[17] in which the damping measured is significantly higher than could be caused by viscoelastic damping. It is probably true that any mathematical model of damping for STEMs may not duplicate the real situation.

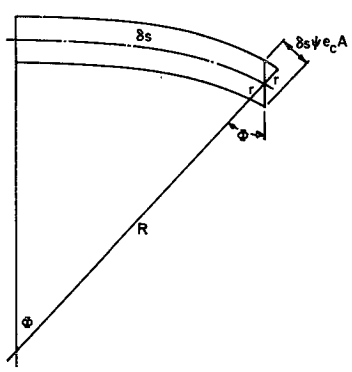

Fig. 3 STEM thermal curvature.

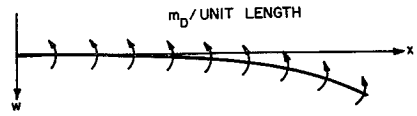

Fig. 4 Distributed damping moment acting on the STEM.

With this in mind, however, it is still felt worthwhile to use a model for damping which does reflect as well as possible the physical situation. It is postulated here that STEM damping is mainly caused by the frictional sliding between overlapped or interlocked sections. As a consequence, the damping moment per unit length at a section is proportional to the time rate of change of curvature of that section. The curvature is used as, in contrast to deflection and slope, it does imply local deformation and hence sliding between the overlapped or interlocked parts. Also, because the action is considered to be one of sliding, the resisting force (and resulting bending moment) must require a finite length to develop. Because of this it is considered preferable to use the concept of damping moment per unit length at a section rather than damping moment per se. In symbols the damping moment per unit length is given by

$$m_D(x) = \eta\dot{w}''$$

where η is the pertinent damping constant for a particular type and section of STEM and is independent of STEM length. Therefore the damping moment at a section x (see Fig. 4) is

$$M_D(x) = \int_x^l m_D(x_1)dx_1$$

$$M_D(x) = \eta \int_x^l \frac{d^2\dot{w}}{dx_1^2}\, dx_1 \quad (18)$$

Using this particular model one result of the ensuing analysis is that, with no thermal excitation, the damping constant is inversely proportional to length. This agrees with the limited comparison made between 28-ft and 43-ft lengths by Predmore.[17]

Stem Motion due to Changing Thermal Curvature

For a beam with thermal curvature K_T, the equation of bending motion including the effect of damping is[13,14]

$$EI(d^2w/dx^2 - K_T) = M_x - M_D \quad (19)$$

Assume a solution for w of the form

$$w(x,\tau) = V(x) + W(x,\tau) \quad (20)$$

where

$$d^2V/dx^2 = \psi e_c \cos\lambda/2r(h + \xi) \quad (21)$$

Then, from Eq. (13)

$$EId^2W/dx^2 - M_x + M_D = EIK_2 \quad (22)$$

where K_2 is the time varying part of the thermal curvature and is given by the inverse transform of the second term of (13).

Mx is the bending moment caused by inertial loads and is given by:

$$Mx = -\mu \int_x^l \ddot{W}(x_1,\tau)(x_1 - x)dx_1 \tag{23}$$

For reasons which will be discussed later, the function u is now introduced where

$$u(x,\tau) = \int_x^l W(x_1,\tau)(x_1 - x)dx_1 \tag{24}$$

and it follows

$$du/dx = -\int_x^l W(x_1,\tau)dx_1 \tag{25}$$

$$d^{n+2}u/dx^{n+2} = d^nW/dx^n,\ n \geq 0$$

and also $Mx = -\mu\ddot{u}$.

Substituting in Eq. (22) and using Eq. (18)

$$\mu\ddot{u} + \eta \int_x^l d^4\dot{u}/dx_1^4(x_1,\tau)dx_1 + EId^4u/dx^4 = EIK_2 \tag{26}$$

Again for reasons of analytical and numerical convenience which are discussed later we change the length variable to y where $y = l - x$ and noting that $d^nu/dx^n = (-1)^nd^nu/dy^n$ leads to

$$\mu\ddot{u} - \eta[\dot{u}'''(0,\tau) - \dot{u}'''(y,\tau)] + EIu'''' = EIK_2 \tag{27}$$

where in Eq. (27) and for the rest of the paper prime denotes differentiation with respect to y, not x.

The boundary conditions on $u(y,\tau)$ are as follows: at $y = 0$, $x = l$ from Eq. (24)

$$u(0,\tau) = 0 \tag{28a}$$

and from Eq. (25)

$$u'(0,\tau) = 0 \tag{28b}$$

Also, at $y = l$, $x = 0$

$$u''(l,\tau) = W(l,\tau) = 0 \tag{28c}$$

and

$$u'''(l,\tau) = W'(l,\tau) = 0 \tag{28d}$$

Equations (28c) and (28d) then reflect the zero deflection and slope at the STEM root. From Eq. (28) the form of the boundary conditions on $u(y,\tau)$ are seen to be precisely the same as the boundary conditions on deflection for a fixed free beam. Also, since the first and third terms in Eq. (27) correspond to those of Euler's beam equation, then advantage can be taken of the tabulated orthogonal characteristic functions[14] to obtain a solution to Eq. (27). This is the case even though physically $u(y,\tau)$ is not a deflection.

This boundary condition convenience is the main reason for utilizing the u function rather than the more conventional approach of differentiating Eq. (22) twice and obtaining the perturbed Euler beam equation with the deflection as the unknown.

The latter approach would need to contend with time varying boundary conditions at the tip and it is extremely important not to neglect these time varying conditions. It is shown in the Appendix that the neglect of these conditions can give a completely erroneous result in the stability criteria.

$u(y,\tau)$ can then be expressed in terms of the infinite series[13,14]

$$u(y,\tau) = \sum_{n=1}^{\infty} X_n(y)fn(\tau) \tag{29}$$

where the X_n are such that

$$EId^4X_n/dy^4 = \mu\omega_n^2X_n \tag{30}$$

Substituting Eqs. (29) and (30) in Eq. (27), multiplying by $X_n(x)$, integrating between 0 and l and using the orthogonal property of the characteristic functions leads to

$$\ddot{f}_n + \omega_n^2f_n + \frac{\eta}{\mu l^3}\sum_{m=1}^{\infty} a_{nm}\dot{f}_m = \frac{EI\int_0^l K_2X_ndy}{\mu\int_0^l X_n^2dy} \tag{31}$$

where

$$a_{nm} = -l^3\frac{\int_0^l [X_m'''(0) - X_m'''(y)]X_n(y)dy}{\int_0^l X_n^2dy} \tag{32}$$

a_{nm} is a constant dependent on the n and m characteristic functions. It is positive for the first few modes at least and, most importantly, is independent of STEM length and other STEM parameters.

For small θ the bracketed term in Eqs. (10) approaches $\theta\sin\lambda$ and

$$\theta = dW/dx$$

$$= -W'$$

Hence

$$\theta = -u''' \tag{33}$$

Taking the Laplace transform of Eq. (31) and using the value of K_2 corresponding to small θ from Eqs. (11) and (13) there is obtained

$$(s + h + \xi)\left[(s^2 + \omega_n^2)F_n(s) + s\left(\frac{\eta}{\mu l^3}\right)\sum_{m=1}^{\infty} a_{nm}F_m(s)\right] - \frac{EI\psi e_c}{2\mu r}\sum_{m=1}^{\infty} b_{nm}F_m(s) = c_n(s + h + \xi) \tag{34}$$

where, it is assumed that $f_n(0) = 0$ and $\dot{f}_n(0) = c_n$ and also

$$b_{nm} = -l^3\left[\int_0^l X_m'''X_n\sin\lambda dy \Big/ \int_0^l X_n^2dy\right] \tag{35}$$

b_{nm} is a constant of the same sign as $\sin\lambda$ for the first few modes at least and is independent of STEM length and other STEM parameters. Now

$$\sin\lambda = \sin(\lambda_0 - \beta)$$

$$= \sin\lambda_0\cos\beta - \cos\lambda_0\sin\beta$$

and since the steady part of the thermal curvature is given by

$$d\beta/ds = K_1 = K_0\cos\lambda$$

So

$$\beta \doteq K_0\cos\lambda_0x$$

Hence to first-order terms in K_0

$$\sin\lambda = \sin\lambda_0 - K_0(l - y)\cos^2\lambda_0 \tag{36}$$

The second term in Eq. (36) will be small except for very long lengths. For such lengths it can be considered in Eq. (35) and hence its effect on the over-all stability determined, but, for this paper, its effect will be neglected.

The amplitudes of the characteristic functions decrease rapidly with increasing n. Hence the stability or otherwise of Eq. (34) should be indicated by considering the term $n = 1$ and only the term $m = 1$ of the summation.

Equation (34) then becomes

$$\left[s^3 + s^2\left(h + \xi + \frac{\eta_1}{\mu l^3}\right) + s\{\omega_1^2 + \frac{\eta_1}{\mu l^3}(h + \xi)\} + (h + \xi)\omega_1^2 - \frac{3.79EI\psi e_c \sin\lambda_0}{2\mu r l^3}\right] F_1(s) = c_1(s + h + \xi) \quad (37)$$

where $\eta_1 = \eta a_{11}$.

a_{11} can be computed from Eq. (32), but it is probably not necessary to do so since any damping measurement will probably comprise the measurement of the logarithmic decrement of a freely oscillating STEM and so η_1 will be measured directly.

Stability of Bending Motion

The criterion of stability is determined by the location of the poles of $F_1(s)$ which are the roots of the cubic in s on the left-hand side of Eq. (37). Being a cubic, the stability or otherwise can be determined by the Routh-Hurwitz criterion.[18]

Firstly, the coefficients of s^3,s^2, and s are positive and

$$\text{Constant Term} = (h + \xi)\omega_1^2 - \frac{3.79EI\psi e_c \sin\lambda_0}{2r\mu l^3}$$

The sign of the constant term provides a static divergence type criterion. Now $\omega_1^2 = 12.35EI/\mu l^4$ (Ref. 13). Hence the constant term is positive for all λ_0 if

$$l < 3.26\ 2r(h + \xi)/\psi e_c$$

or

$$l < 3.26/K_0$$

Typically the value of K_0 for Beryllium Copper STEM is 8×10^{-4} ft^{-1}

Hence the constant term is positive for all λ_0 if $l < 4000$ ft, implying that the constant term is positive for the range of l with which we are dealing and hence no static divergence occurs. In addition, for stability the appropriate matrix of the coefficients must be positive and this leads to the stability criterion for dynamic flutter.

$$\eta_1\left[\omega_1^2 + \left(\frac{\eta_1}{\mu l^3}\right)(h + \xi) + (h + \xi)^2\right] > -\frac{3.79EI\psi e_c \sin\lambda_0}{2r} \quad (38)$$

For $\eta_1 = 0$ then, the STEM is unstable for $-(\pi/2) < \lambda_0 < 0$ and stable for $0 < \lambda_0 < (\pi/2)$. This indicates that the sun provides a destabilizing influence if the STEM is directed away from it and a stabilizing influence if the STEM is directed towards it.

The third term on the left-hand side of Eq. (38) is independent of length and using it alone, it can be seen that if

$$\eta_1 > -\frac{3.79EI\psi e_c \sin\lambda_0}{2r(h + \xi)^2} \quad (39)$$

then the STEM is stable for all lengths.

The second term is small compared to the other two and can be neglected whereas the first term is of the order of $(1/l^4)$ and so is increasingly important at shorter lengths. Using the following values: $S = 450$ Btu/hr ft^2, $e_c = 1.04 \times 10^{-5}$/°F, $c = 3.2$ Btu/slug ft^2, and using the following values for 0.5-in.-diam BeCu STEM: $EI = 15$ lb ft^2, $\mu = 4.4 \times 10^{-4}$ slug/ft, $r = 0.25$ in., $t = 0.002$ in., and $k = 44$ Btu/hr ft°F, then these can be computed:

$$\psi = 11.6\alpha,\ \xi = 0.44,\ h = 0.004$$

and the STEM is stable for all lengths if

$$\eta_1 > -0.85\alpha \sin\lambda_0 \quad (40)$$

A nominal value of α for unplated STEM is 0.4 and for Ag-plated STEM is 0.12. Some limited testing on damping[17] has been carried out on 28-ft and 43-ft lengths of overlapped STEM. There is a great deal of uncertainty as to how applicable the results are and, as pointed out later, much better damping information is required. However, one would expect the order of magnitude of damping to be about the same as that reported in these tests. The range of values reported for the damping constant was $\zeta = 0.0013$ to 0.0075.

Also it was observed that in the limited comparison that could be made between the 28-ft and 43-ft lengths, the damping constant tended to be inversely proportional to length.

Examination of Eq. (37) without the thermal terms leads to

$$s^2 + (\eta_1/\mu l^3)s + \omega_1^2 = c_1$$

and hence the damping constant can be found from

$$2\zeta\omega_1 = \eta_1/\mu l^3$$

and since

$$\omega_1^2 = 12.35EI/\mu l^4$$

then

$$\zeta = \eta_1/7.02l(EI\mu)^{1/2} \quad (41)$$

thus confirming the preceding tentative experimental observation regarding the variation of damping constant with length.

Using these values for 0.5-in.-diam beryllium copper STEM, Table 1 has been constructed to determine the stability or otherwise of this STEM, both with and without silver plating. The required value of η_1 is obtained from Eq. (40). λ_0 is assumed to be $-60°$, the latter being an estimate of the most unfavorable practical orientation likely to last for an extended period. Since most damping tests[17] have been based on 43-ft-lengths, then the required damping constant for this length is computed from Eq. (41). If this is less than the actual damping constant measured, then the STEM is stable for all lengths. If less than the maximum length for stability, it can be determined by using the first term of Eq. (38). The upper and lower limits for ζ are listed in Table 1 and the stability criterion is determined for each limit.

The table indicates that there are always unstable lengths for unplated STEM no matter where the damping value may lie within the reported range. However, for silver-plated STEM the occurrence of instability is very sensitive to the actual damping value. It should be recognized of course that, because of the degree of uncertainty regarding damping, these conclusions can only be made in a qualitative sense. Suffice it to say that there is a distinct probability that such an unstable oscillation could occur on a spacecraft should the sun orientation be sufficiently unfavorable. More damping tests should be carried out to obtain better damping values. However, any results would need to be considered in the light of the probability that such values may vary from unit to unit. Also, the value for any one unit may change over time

Table 1 Stability of 0.5-in.-diam BeCu STEM, $\lambda_0 = -60°$

Surface	Solar absorptivity α	Required η_1	Required ζ for $l = 43$ ft	Measured ζ for $l = 43$ ft	Stability
Unplated	0.4	0.294	0.012	0.0013	Stable for $l < 22$ ft
Unplated				0.0075	Stable for $l < 43$ ft
Silver plated	0.12	0.088	0.0036	0.0013	Stable for $l < 33$ ft
Silver plated				0.0075	Stable for all l

in space due to element relaxation and the wear effects of friction in the overlapped or interlocked parts.

Conclusion

This investigation has lead to criteria for the stability of STEM oscillations in bending in the plane of the sun. The mechanism for the excitation of such an oscillation has been derived taking into account the major modes of heat transfer operating and the dynamics of the system. The temperature differentials caused by the sun have been shown to cause a stabilizing effect when the STEM is pointing into the sun and a destabilizing effect when the STEM is pointing away from the sun.

The major source of damping present is that due to friction in the overlapping portion of the STEM. Numerical investigation using the best test values available for this type of damping has shown that stability is marginal for silver-plated STEM and that the oscillation will be unstable for all but short lengths of unplated STEM. It is important to obtain accurate values of damping constant for the various types of interlocked STEM in order to determine finally the stability or otherwise of these configurations that now appear marginal.

Appendix: Discussion of Formulation of Stability Criteria

The equation of the system was set up in terms of the function $u(y,\tau)$ rather than the deflection $W(x,\tau)$ [see Eqs. (24) and (26)]. The reason is discussed below.

Neglecting the damping term, Eq. (22) can be differentiated twice to give

$$EId^4W/dx^4 + \mu\ddot{W} = EId^2K_2/dx^2 \tag{A1}$$

where W is the time varying component of the deflection and K_2 is the time varying component of the thermal curvature.

The boundary conditions on W are
At fixed end,

$$x = 0,\ W(0,\tau) = 0 \tag{A2a}$$

$$dW/dx(0,\tau) = 0 \tag{A2b}$$

At free end,

$$x = l,\ d^2W/dx^2(l,\tau) = K_2(l,\tau) \tag{A2c}$$

$$d^3W/dx^3(l,\tau) = dK_2/dx(l,\tau) \tag{A2d}$$

In contrast to the boundary conditions Eq. (28) on u these differ in the inclusion of tip thermal curvature in Eq. (A2c) and Eq. (A2d). Hence the direct use of the tabulated fixed free beam characteristic functions is precluded and either new characteristic functions need to be computed or some other method devised. It is important to include this particular tip thermal curvature to obtain the correct result. If it is ignored by putting the right-hand sides of Eq. (A2c) and (A2d) equal to zero and if one used the same characteristic function approach as was done for u, then instead of Eq. (33) which is $\theta = -u'''$ there will be obtained instead

$$\theta = d^3W/dx^3 \tag{A3}$$

Hence, at this point a sign reversal is introduced which leads to a reversal in sign of the last term of the left-hand side of Eq. (37). Hence, the stability criterion is completely reversed.

References

[1] Donohue, J. H. and Frisch, H. P., "Thermoelastic Instability of Open Section Booms," Symposium on Gravity Gradient Attitude Control, Dec. 1968, sponsored by the Air Force (SAMSO) and Aerospace Corp., Los Angeles, Calif.

[2] Foulke, H., "Effect of Thermal Flutter On Gravity Gradient Stabilized Spacecraft," Symposium on Gravity Gradient Attitude Control, Dec. 1968, sponsored by the Air Force (SAMSO) and Aerospace Corp., Los Angeles, Calif.

[3] Raymond, F. W., Wilhelm, P. G., and Beal, R. T., "Gravity Gradient Flight Experience Acquired With The Naval Research Lab. Satellites," Symposium on Gravity Gradient Attitude Control, Dec. 1968, sponsored by the Air Force (SAMSO) and Aerospace Corp., Los Angeles, Calif.

[4] Connell, G. M. and Chobotov, V., "Possible Effects of Boom Flutter on the Attitude Dynamics of the OV1-10 Satellite," *Journal of Spacecraft and Rockets*, Vol. 6, No. 1, Jan. 1969, pp. 90–92.

[5] Frisch, H. P., "Thermally Induced Vibrations of Long Thin-Walled Cylinders of Open Section," *ASME/AIAA 10th Structures, Structural Dynamics and Materials Conference*, AIAA, New York, 1969.

[6] Rimrott, F. P. J., "Storable Tubular Extendible Member," *Machine Design*, Vol. 37, No. 28, 1965, pp. 156–165.

[7] Koval, L. R., Mueller, M. R., and Paroczai, A. J., "Solar Flutter of A Thin-Walled Open-Section Boom," Symposium on Gravity Gradient Attitude Control, Dec. 1968, sponsored by the Air Force (SAMSO) and Aerospace Corp., Los Angeles, Calif.

[8] Graham, J. D., "The Analysis of The Small Angle Twist Response of A Slit Tube To Solar Radiation," Internal Reports TM 640 and TM 642, Dec. 1968, Spar Aerospace Products Ltd., Malton, Ontario, Canada.

[9] Grimshaw, E. R. and Wells, A., "Gravity Gradient Booms —Their Origin and Evolution," Symposium on Gravity Gradient Attitude Control, Dec. 1968, sponsored by the Air Force (SAMSO) and Aerospace Corporation, Los Angeles, Calif.

[10] Yu, Y.-Y., "Thermally Induced Vibration and Flutter of A Flexible Boom," AIAA Paper 69-21, New York, 1969.

[11] Farrell, K., Kemper, A., and MacNaughton, J. D., "Temperature Gradients and Profile Changes In Long Tubular Elements Due to Incident Radiation," Rept. DHC-SP-TN.164, Dec. 1962, prepared for Naval Research Labs. by SPAR Div., de Havilland Aircraft of Canada.

[12] Florio, F. A. and Hobbs, R. B., Jr., "Analytical Representation of Temperature Distributions in Gravity Gradient Rods," *AIAA Journal*, Vol. 6, No. 1, Jan. 1968, pp. 99–102.

[13] Volterra, E. and Zachmanoglou, E. C., *Dynamics of Vibrations*, Charles E. Merrill, Columbus, Ohio, 1965, pp. 319–320, 327–329.

[14] Thomson, W. T., *Vibration Theory and Applications*, Prentice-Hall, Englewood Cliffs, N.J., 1965, pp. 273–276, 353–360.

[15] Likins, P. W., "Modal Method for Analysis of Free Rotations of Spacecraft," *AIAA Journal*, Vol. 5, No. 7, July 1967, pp. 1304–1308.

[16] Zener, C., *Elasticity and Anelasticity of Metals*, The University of Chicago Press, Chicago, 1948.

[17] Predmore, R. E., Staugaitis, C. L., and Jellison, J. E., "Damping Behaviour of DeHavilland STEM Booms," TN D-3966, June 1967, NASA.

[18] Kuo, B. C., *Automatic Control Systems*, Prentice-Hall, Englewood Cliffs, N.J., 1964, pp. 156–163.